Journal of Solid State Chemistry **155,** 298–304 (2000)
doi:10.1006/jssc.2000.8899, available online at http://www.idealibrary.com on IDEAL®

Crystal Structure and Phase Transitions in *N*-benzyl Piperidinium Dihydrogenmonophosphate, $C_6H_5CH_2CHCH_2CH_2NH_2CH_2CH_2 \cdot H_2PO_4$

Z. Elaoud,* S. Kamoun,* T. Mhiri,†,[1] F. Romain,‡ and H. Burzlaff§

*Laboratoire de Cristallochimie du Solide, ENIS, 3038 Sfax, Tunisia; †Laboratoire de l'Etat Solide, Département de Chimie, Faculté des Sciences de Sfax, 3038 Sfax, Tunisia; ‡Laboratoire de Dynamique, Interaction, Réactivité, CNRS, 2 rue Henry Dunant, 94320 Thiais, France; and §Institut für Angewandte Physik, Lehrstuhl für Kristallographie, Universität Erlangen, Bismarckstrasse 10, D-91054 Erlangen, Germany

Received April 17, 2000; in revised form July 6, 2000; accepted July 28, 2000; published online November 29, 2000

The salt *N*-benzyl piperidinium dihydrogenmonophosphate (N-BPP) is orthorhombic $P2_12_12_1$ with the following unit cell dimensions: $a = 6.044(1)$ Å, $b = 9.038(1)$ Å, $c = 25.126(3)$ Å, $D_m = 1.302$ Mg m^{-3}, $D_x = 1.322$ Mg m^{-3}, $\mu = 0.21$ mm^{-1}, $F(000) = 584$; $T = 298$ K; $R = 0.045$, and $R_w = 0.138$ for 1721 independent reflections. The structure consists of infinite parallel two-dimensional planes built of mutually $H_2PO_4^-$ anions and $[C_6H_5CH_2CHCH_2CH_2NH_2CH_2CH_2]^+$ cations connected by strong O–H ··· O and N–H ··· O hydrogen bonding. There are no contacts other than normal van der Waals interactions between the layers. Differential scanning calorimetry study on N-BPP was carried out. A low-temperature phase transition at 269 K to an ordered phase was found. Measurements by the electric permittivity revealed a second-order phase transition at 269 K. The Raman and infrared of polycrystalline samples of N-BPP have been recorded at different temperatures between 170 and 435 K. © 2000 Academic Press

Key Words: **structure; phase transitions; vibrational spectroscopy; dielectric measurements.**

I. INTRODUCTION

During a systematic investigation of interaction between monophosphoric acid and organic molecules numerous structures of monophosphate salts have been described: $[NH_3(CH_2)_2NH_2(CH_2)_2NH_2(CH_2)_2NH_3](HPO_4)_2 \cdot 2H_2O$(1), $NH_3(CH_2)_2NH_3(H_2PO_4)_2$ (2, 3), $NH_3(CH_2)_3NH_3(H_2PO_4)_2$ (4), $NH_3(CH_2)_3NH_3HPO_4 \cdot H_2O$ (5), $NH_3(CH_2)_4NH_3HPO_4 \cdot 2H_2O$(6), $[NH_3(CH_2)_2]_2NH \cdot HPO_4 \cdot 2H_2O$ (7, 8), $C_6H_5CH_2NH_2CH_3 \cdot H_2PO_4 \cdot H_2O$(9). In the present work we describe the crystal structure of the *N*-benzyl piperidinium dihydrogenmonophosphate (hereafter abreviated to N-BPP). Detailed calorimetric, dielectric, and vibrational spectroscopy features are given.

II. EXPERIMENTAL DETAILS

II.1. Crystal Chemistry

Colorless crystals of N-BPP were grown in two stages: first, a batch of seed material was prepared from an aqueous solution containing a stoichiometric mixture of *N*-benzyl piperidine $C_6H_5CH_2CHCH_2CH_2NH_2CH_2CH_2$ and monophosphoric acid H_3PO_4, second, the growth of nuclei to desired dimensions was carried out by slow evaporation of the solvent at constant temperature (25°C). The chemical analysis of phosphorus and acidic protons has been carried out (10). The N-BPP salt crystallizes in the orthorhombic $P2_12_12_1$ system with the following unit cell dimensions: $a = 6.044(1)$ Å, $b = 9.038(1)$ Å, $c = 25.126(3)$ Å. The unit cell dimensions were obtained from a least squares refinement based on 25 reflections accurately centered by the goniometer. Density was measured at room temperature by flotation in tetrachlorobenzene. The average value of density, $D_m = 1.302$ Mg m^{-3}, is in agreement with that calculated, $D_x = 1.322$ Mg m^{-3}. The cell contains four formula units of $C_6H_5CH_2CHCH_2CH_2NH_2CH_2CH_2 \cdot H_2PO_4$.

II.2. Crystal Structure

Experimental conditions used for the single crystal diffraction data collection are reported in the Table 1. Unit cell parameters were refined using sets of 25 reflections in the range $2.11 \leq \theta \leq 27°$. The crystal had the parallelipipedic form with a size of about $(0.18 \times 0.24 \times 0.48)$ mm^3. A small specimen was selected with an Enraf-Nonius CAD-4 diffractometer using Mo$K\alpha$ radiation $\omega - 2\theta$ scan mode. The scan width was $1 + 0.35 \operatorname{tg}\theta°$; 2325 reflections with miller indices $0 \leq h \leq 35$, $0 \leq k \leq 12$, $0 \leq l \leq 8$ were collected.

[1] To whom correspondence should be addressed.

0022-4596/00 $35.00

TABLE 1
Crystal Data and Summary of Intensity Data Collection and Structure Refinement

Compound	$C_6H_5CH_2CHCH_2CH_2NH_2CH_2CH_2 \cdot H_2PO_4$
Color/shape	Colorless/papallelipiped
Molecular weight ($g\,mol^{-1}$)	273.26
Space group	$P2_12_12_1$
Temp. (°C)	25
Cell constants[a]	
a (Å)	6.044(1)
b (Å)	9.038(1)
c (Å)	25.126(3)
Cell volume (Å^3)	1372.52
Formula units /unit cell	4
D_{calc} (g cm^{-3})	1.322
μ_{calc} (cm^{-1})	2.1
Diffractometer/scan	Enraf Nonius CAD4/$\omega - 2\theta$
Radiation, graphite monochromater	Mo$K\alpha$ ($\lambda = 0.71070$ Å)
Max. crystal dimensions (mm)	$0.18 \times 0.24 \times 0.48$
Decay of standards	$\pm 4\%$
Reflections measured	2325
Range of h, k, l	0/35, 0/12, 0/8
Reflections with $F_0 > 4\sigma(F_0)$[b]	1721
$F(000)$	584
Weights	$1/(\sigma^2(F_0^2) + (0.0367P)^2 + 1.57P)$ $P = (F_0^2 + 2F_c^2)/3$
GOF	0.924
$R = \sum\|\|F_0\| - \|F_c\|\|/\sum\|F_0\|$	0.0447
Rw	0.1375
Largest feature final diff. map	0.05 e/Å^3
Computer programs[c]	SHELXS(11), SHELXL(12)

[a]Least-squares refinement based on 25 reflections.
[b]Corrections: Lorentz polarization.
[c]Neutral scattering factors and anomalous dispersion corrections.

Two standard reflections (-313 and -1–2–12) with no systematic variation were observed. Lorentz and polarization corrections have been made. The crystal structure has been solved using the classical method: interpretation of the three-dimensional Patterson function followed by successive difference Fourier maps after introducing anisotropic thermal factors for the nonhydrogen atoms and isotropic ones for H atoms. The final refinement cycles with reflections 1721 corresponding to the criterion $F_0 > 4\sigma(F_0)$ yield $R = 0.045$ and Rw $= 0.138$. All calculations were performed on PC computer using SHELXS 86 (11) and SHELXL 93 (12) packages.

II.3. Differential Scanning Calorimetry

DSC measurements were performed on heating samples from 150 to 580 K on a Setaram apparatus (Model DSC 92) at a heating rate of 5 K min^{-1}

II.4. Dielectric Measurements

A polycrystalline sample of N-BPP was pressed at room temperature under 200 MPa stress. Dense pellets of 1 cm diameter and 1 mm thickness were obtained. Metallic silver was deposited on both sides which served as electrodes. The dielectric measurements versus temperature (150–400 K) were performed at 1 kHz frequency using a Hewlett-Packard 4192ALF automatic bridge monitored by a HP vectra microcomputer. The measurements were carried out in vacuum.

II.5. Spectroscopic Measurements

Raman spectra of polycrystalline samples sealed in a glass tube were recorded on a DILOR RTI 30 (triple mono-

TABLE 2
Atomic Coordinates and U_{eq} or U_{iso} for $C_6H_5CH_2CHCH_2CH_2NH_2CH_2CH_2 \cdot H_2PO_4$. $U_{eq} = \frac{1}{3}\sum_i\sum_j U_{ij}\, a_i^* a_j^* a_i a_j$

Atoms	x/a	y/b	z/c	U_{eq} or U_{iso}^*(Å)
P	0.7222(2)	0.9063(1)	0.02076(5)	0.0347(3)
O(1)	0.7227(6)	0.8098(3)	−0.0285(1)	0.0428(8)
O(2)	0.9564(6)	0.9101(5)	0.0480(1)	0.0557(11)
O(3)	0.6611(7)	1.0643(3)	0.0119(1)	0.0544(10)
O(4)	0.5696(8)	0.8364(5)	0.0641(1)	0.0577(12)
N	0.9002(7)	1.2880(5)	0.0574(2)	0.0404(10)
C(1)	1.0666(10)	1.2476(6)	0.0993(2)	0.0450(12)
C(2)	1.1395(9)	1.3856(5)	0.1287(2)	0.0400(11)
C(3)	0.9435(9)	1.4670(5)	0.1534(2)	0.0387(11)
C(4)	0.7759(10)	1.5040(6)	0.1100(2)	0.0455(12)
C(5)	0.7052(9)	1.3664(6)	0.0798(2)	0.0453(12)
C(6)	1.0165(9)	1.6085(6)	0.1822(2)	0.0475(12)
C(7)	1.1718(10)	1.5868(6)	0.2288(2)	0.0475(13)
C(8)	1.1158(11)	1.4972(6)	0.2716(2)	0.0514(14)
C(9)	1.2569(12)	1.4791(6)	0.3151(2)	0.0552(15)
C(10)	1.4564(12)	1.5507(8)	0.3158(3)	0.0637(19)
C(11)	1.5148(12)	1.6399(9)	0.2739(3)	0.0696(20)
C(12)	1.3755(12)	1.6581(7)	0.2306(2)	0.0577(16)
H(O2)	1.04210	0.82643	0.04165	0.1038*
H(O4)	0.47571	0.78905	0.05213	0.0450*
H(1N)	0.85602	1.20116	0.04154	0.0277*
H(2N)	0.97099	1.36173	0.01933	0.0581*
H(1C1)	1.01396	1.17675	0.12135	0.0621*
H(2C1)	1.18761	1.20023	0.08158	0.0709*
H(1C2)	1.25162	1.35332	0.15411	0.0426*
H(2C2)	1.21302	1.45643	0.10563	0.0348*
H(1C3)	0.87942	1.39707	0.18003	0.0333*
H(1C4)	0.84190	1.57547	0.08243	0.0612*
H(2C4)	0.64944	1.55201	0.12453	0.0700*
H(1C5)	0.60436	1.38827	0.05034	0.0530*
H(2C5)	0.64005	1.29858	0.10337	0.0520*
H(1C6)	1.07105	1.67116	0.15708	0.0619*
H(2C6)	0.87008	1.66852	0.19371	0.0645*
H(1C8)	0.99554	1.44906	0.27201	0.0530*
H(1C9)	1.20387	1.41263	0.34517	0.0826*
H(1C10)	1.56107	1.53263	0.34599	0.0647*
H(1C11)	1.64757	1.69693	0.27265	0.1154*
H(1C12)	1.41375	1.71881	0.20311	0.0645*

chromator instrument) monitored by a Tandon microcomputer and equipped with an argon ion laser (Spectra Physics Model 2025; $\lambda_{exc} = 514.5$ nm). The samples was cooled in a gas convection cryostat, using liquid nitrogen as coolant. A temperature stability of about ± 1 K was achieved. Infrared spectra were studied with Perkin Elmer 980 spectrometer. The polycrystalline product was examined as an emulsion in Nujol between ICs facets. A conventional nitrogen cryostat was employed for the IR measurements.

III. RESULTS AND DISCUSSION

III.1. X-Ray Diffraction Study

The final coordinates and U_{eq} or U_{iso} are given in Table 2. Interatomic distances, bond angles, and the hydrogen bonding are listed in Table 3. Anisotropic thermal parameters for the nonhydrogen atoms are reported in Table 4. The projection of the atomic arrangement of N-BPP viewed down the *a* axis is shown in Fig. 1. The structure consists of infinite parallel two-dimensional planes built of mutually connected ions $H_2PO_4^-$ tetrahedra and $[C_6H_5CH_2\underline{CHCH_2CH_2NH_2CH_2CH_2}]^+$ cations. The $H_2PO_4^-$ tetrahedra are associated in pairs forming noncentrosymmetric finite clusters $[H_4P_2O_8]^{2-}$. The P–P distance between two $H_2PO_4^-$ groups linked by four hydrogen bonds is 4.267 Å. The P–O distances range from 1.492 to 1.573 Å. These values are comparable to the reported date (3, 6–8, 13). The longest P–O distances, 1.560 and 1.573 Å, are due to the presence of the acidic hydrogen atoms on the PO_4 tetrahedron. These pairs are extented to a two-dimensional

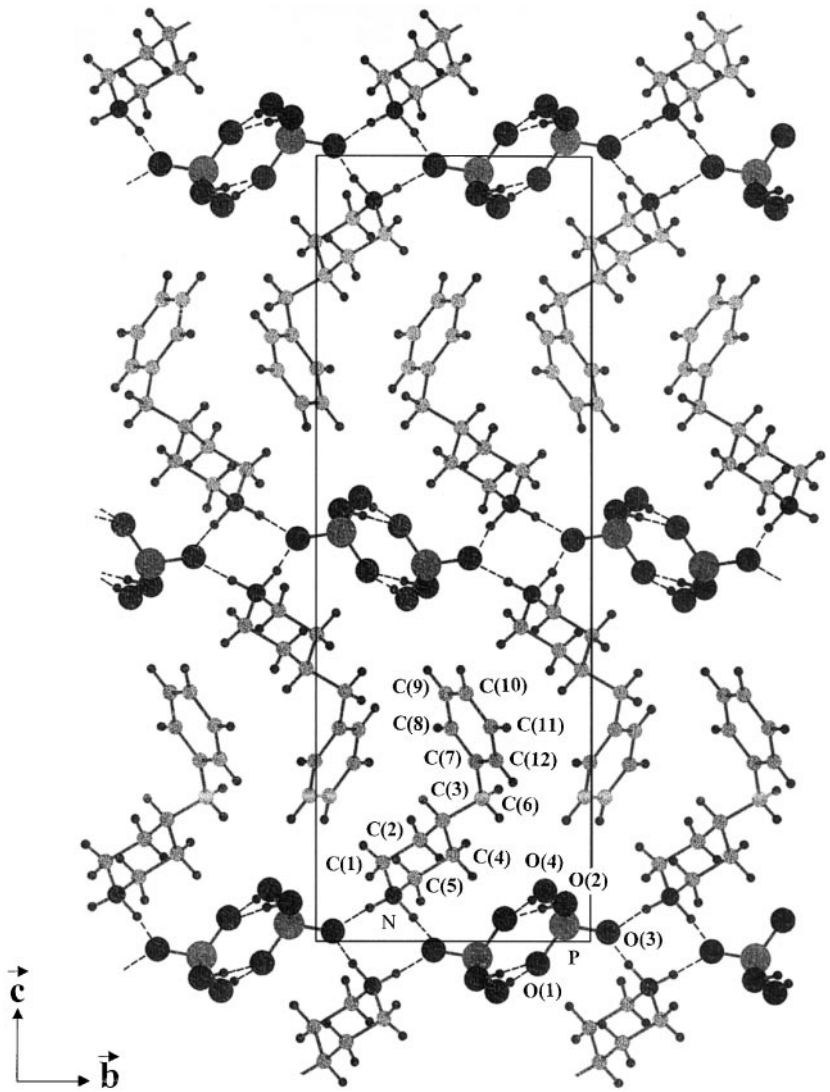

FIG. 1. Projection along the *a* axis of the atomic arrangement of $C_6H_5CH_2\underline{CHCH_2CH_2NH_2CH_2CH_2} \cdot H_2PO_4$. The broken lines show the hydrogen bonding.

TABLE 3
Principal Intermolecular Distances (Å) and Bond Angles (°) and the Detailed of the Hydrogen Bonding Scheme in $C_6H_5CH_2CHCH_2CH_2NH_2CH_2CH_2 \cdot H_2PO_4$

P	O(1)	O(2)	O(3)	O(4)
O(1)	1.514(3)	111.54(20)	115.46(20)	111.54(20)
O(2)	111.54(20)	1.573(4)	105.48(22)	103.70(24)
O(3)	115.46(20)	105.48(22)	1.492(3)	110.22(25)
O(4)	111.54(20)	103.70(24)	110.22(25)	1.560(4)

P–O(2)–H(O2): 114.06
P–O(4)–H(O4): 112.87
O(2)–H(O2): 0.931
O(4)–H(O4): 0.771

$[C_6H_5CH_2CHCH_2CH_2NH_2CH_2CH_2]^+$

C(1)–C(2): 1.515(7)	N–C(1)–C(2):109.67(42)
N–C(1):1.501(7)	C(1)–N–C(5):112.41(40)
N–C(5):1.486(7)	C(1)–C(2)–C(3):111.65(45)
C(2)–C(3):1.527(7)	C(2)–C(3)–C(4):109.19(39)
C(3)–C(4):1.525(7)	C(4)–C(3)–C(6):110.36(42)
C(3)–C(6):1.535(7)	C(3)–C(4)–C(5):111.61(43)
C(4)–C(5):1.514(7)	N–C(5)–C(4):110.89(45)
C(5)–N:1.486(7)	C(3)–C(6)–C(7):115.79(44)
C(6)–C(7):1.513(7)	C(8)–C(7)–C(6):121.60(52)
C(7)–C(8):1.389(7)	C(8)–C(7)–C(12):117.46(54)
C(7)–C(12):1.390(8)	C(12)–C(7)–C(6):120.93(50)
C(8)–C(9):1.395(8)	C(7)–C(8)–C(9):121.71(62)
C(9)–C(10):1.368(9)	C(10)–C(9)–C(8):119.59(59)
C(10)–C(11):1.372(10)	C(11)–C(10)–C(9):119.62(63)
C(11)–C(12):1.386(9)	C(10)–C(11)–C(12):121.08(69)
N–H(1N):0.919(44)	C(11)–C(12)–C(7):120.53(62)
N–H(2N):1.060(55)	C(6)–C(3)–H(1C3):109(2)
C(1)–H(1C1):0.904(57)	C(2)–C(3)–H(1C3):106(3)
C(1)–H(2C1):0.957(65)	C(4)–C(3)–H(1C3):111(3)
C(2)–H(1C2):0.976(52)	
C(2)–H(2C2):0.971(46)	
C(3)–H(1C3):0.998(45)	
C(4)–H(1C4):1.030(55)	
C(4)–H(2C4):0.954(63)	
C(5)–H(1C5):0.979(55)	
C(5)–H(2C5):0.939(56)	
C(6)–H(1C6):0.910(56)	
C(6)–H(2C6):1.078(62)	
C(8)–H(1C8):0.847(61)	
C(9)–H(1C9):1.018(63)	
C(10)–H(1C10):1.001(59)	
C(11)–H(1C11):0.955(85)	
C(12)–H(1C12):0.912(55)	

Hydrogen bonds

	D–H	H ⋯ A	D ⋯ A	D–H ⋯ A
O(2)–H(O2) ⋯ O(1)^{i}	0.931(76)	1.678(77)	2.604(5)	173(7)
O(4)–H(O4) ⋯ O(1)^{ii}	0.771(56)	1.868(58)	2.635(5)	172(6)
N–H(1N) ⋯ O(3)	0.919(44)	1.864(47)	2.735(5)	157(4)
N–H(2N) ⋯ O(3)^{iii}	1.060(55)	1.685(58)	2.701(6)	159(5)

Note. Symmetry code: (i) $\frac{1}{2}+X, \frac{3}{2}-Y, -Z$, (ii) $-\frac{1}{2}+X, \frac{3}{2}-Y, -Z$, (iii) $\frac{1}{2}+X, \frac{5}{2}-Y, -Z$.

network by the hydrogens of the N-atom at positions $x = 0.25$ and 0.75.

The organic groups are located in the [011] planes at $x = 0.5$. Table 3 reports the principal geometrical features of the $[C_6H_5CH_2CHCH_2CH_2NH_2CH_2CH_2]^+$cations. They are in agreement with these found in related compound (9,14–17). The C–C perpendicular interplanar distances ranges from 4.096 to 8.24 Å, indicating the existence of strong interaction by van der Waals contacts between $[C_6H_5CH_2CHCH_2CH_2NH_2CH_2CH_2]^+$ cations. All the hydrogen bonds (D–H ⋯ A) and the van der Waals contacts give rise to three-dimensional network in the structure and add stability to this compound.

III.2. Phase Transition in N-BPP

III.2.1. Differential scanning calorimetry. DSC experiments were performed on heating N-BPP samples from 150 to 580 K. The thermal analysis result is reported in Fig. 2. The thermogram shows two endothermic peaks at $T_1 = 269$ K and $T_2 = 502$ K. The enthalpy and entropy changes are, respectively, $\Delta H_1 = 0.385\ \text{kJ mol}^{-1}$ and $\Delta S_1 = 1.43\ \text{J mol}^{-1}\,\text{K}^{-1}$. The first transition observed at 269 K is reversible. For this transition, the relation $\Delta S = R \ln \Omega$ brings to a number of equivalent positions $\Omega = 1.18$. This transition may be interpreted by a dynamic order–disorder. The second transition observed at 500 K corresponds to the melting of the N-BPP. The melting enthalpy and entropy are, respectively, $\Delta H_2 = 51.340\ \text{kJ mol}^{-1}$ and $\Delta S_2 = 102.68\ \text{J mol}^{-1}\,\text{K}^{-1}$.

III.2.2. Dielectric studies. In order to give more information on the crystal dynamics (short interaction distance), we have undertaken a dielectric study between 150 and 400 K. Figure 3 shows the thermal variation of both the permittivity ε'_r and the dielectric losses $\tan\delta$. One maximum of ε'_r appears at 269 ± 2 K. A maximum of ε'_r corresponding to a maximum of $\tan\delta$ is observed. This dielectric behavior rules out the existence of a ferroelectric phase at the low temperature.

III.2.3. Raman and IR spectroscopic studies. Vibrational spectroscopy has been widely used in the study of structural phase transitions of a number of crystals and can give useful informations about phases and their transformations (17–21). In our opinion, Raman spectroscopy is well suited for the study of the dynamics of the lattice vibrational modes. The aim of this investigation is to present Raman and IR spectra of the N-BPP salt as function of temperature in the region covering its phase transitions (170–435 K). We wish to confirm the established nature of the (II → I) phase transition and add some new data dealing with the disorder of the room temperature phase (I).

TABLE 4
Anisotropic Thermal Parameters for $C_6H_5CH_2CHCH_2CH_2NH_2CH_2CH_2 \cdot H_2PO_4$.

$$T = \exp\text{-}(U_{11}h^2 + U_{22}k^2 + U_{33}l^2 + 2U_{12}hk + 2U_{13}hl + 2U_{23}kl)$$

Atoms	U_{11}	U_{22}	U_{33}	U_{12}	U_{13}	U_{23}
P	0.0340(6)	0.0307(5)	0.0393(5)	0.0004(5)	− 0.0069(5)	− 0.0049(5)
O(1)	0.0359(17)	0.0464(16)	0.0461(17)	− 0.0053(16)	0.0002(17)	− 0.0127(14)
O(2)	0.0428(22)	0.0568(21)	0.0675(23)	0.0133(22)	− 0.0237(20)	− 0.0274(21)
O(3)	0.0634(25)	0.0357(17)	0.0640(22)	0.0028(17)	− 0.0285(20)	− 0.0009(15)
O(4)	0.0641(28)	0.0712(26)	0.0379(19)	− 0.0263(25)	− 0.0043(20)	− 0.0058(18)
N	0.0396(24)	0.0378(20)	0.0437(22)	− 0.0067(20)	− 0.0002(20)	− 0.0034(18)
C(1)	0.0483(33)	0.0383(24)	0.0483(28)	0.0021(27)	− 0.0041(27)	0.0010(23)
C(2)	0.0373(25)	0.0388(25)	0.0440(25)	0.0024(23)	− 0.0052(23)	− 0.0003(21)
C(3)	0.0431(29)	0.0378(22)	0.0352(22)	− 0.0020(24)	0.0041(23)	0.0030(19)
C(4)	0.0381(28)	0.0475(25)	0.0508(28)	0.0085(27)	− 0.0013(27)	− 0.0028(23)
C(5)	0.0335(25)	0.0551(30)	0.0474(26)	− 0.0011(26)	− 0.0037(25)	0.0007(23)
C(6)	0.0565(34)	0.0397(26)	0.0462(27)	0.0004(29)	0.0027(27)	0.0006(24)
C(7)	0.0514(31)	0.0388(22)	0.0412(23)	0.0008(28)	0.0057(23)	− 0.0070(22)
C(8)	0.0529(36)	0.0459(28)	0.0555(32)	− 0.0066(30)	0.0012(31)	− 0.0049(25)
C(9)	0.0683(42)	0.0529(28)	0.0445(27)	0.0004(34)	− 0.0051(32)	− 0.0093(24)
C(10)	0.0654(42)	0.0806(45)	0.0451(30)	0.0034(39)	− 0.0089(33)	− 0.0208(30)
C(11)	0.0549(39)	0.0901(51)	0.0637(37)	− 0.0190(39)	0.0022(39)	− 0.0258(36)
C(12)	0.0654(40)	0.0652(34)	0.0424(28)	− 0.0177(34)	0.0114(31)	− 0.0102(28)

Thermal evolution of Raman spectra are shown in Figs. 4A–C. When the temperature is increased from 175 to 433 K, the Raman spectra show a noticeable frequency shift of most the observed external bands. Analysis of these bands shows that there are few vibrations such as the bands appearing at 175 K at 99, 106, 113, and 126 cm^{-1} which coalexe when the sample was heated above the transition temperature 269 K. The wave numbers of the Raman lines (external phonons) are continuously decreasing with the increasing temperature: this is in agreement with the disorder introduced by the anti-ferroelectric phase at room temperature. A systematic temperature dependence study of some halfwidths $\Delta\nu_{1/2}$ (Fig. 5) shows clearly one phase

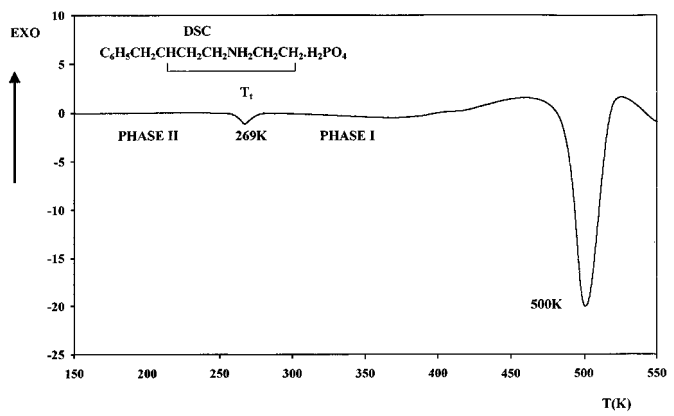

FIG. 2. Differential scanning calorimeter run on $C_6H_5CH_2CHCH_2CH_2NH_2CH_2CH_2 \cdot H_2PO_4$.

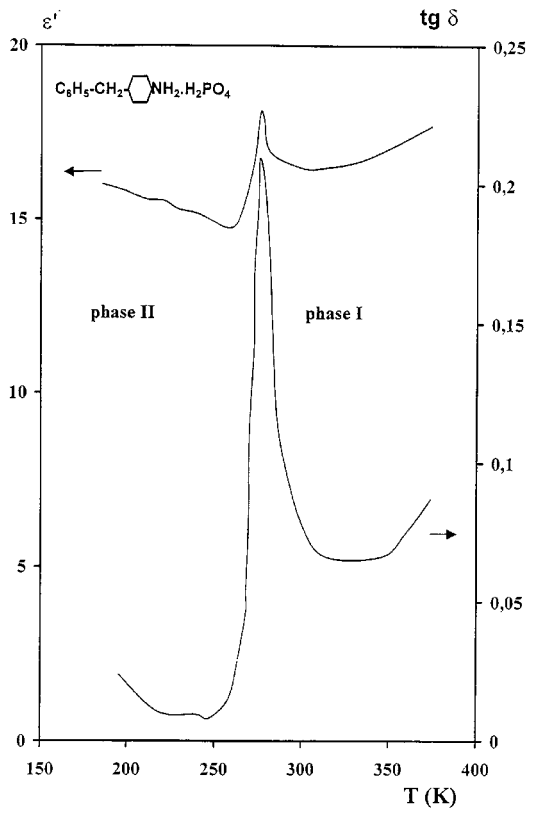

FIG. 3. Thermal variation of ε'_r and $\tan\delta$ for $C_6H_5CH_2CHCH_2CH_2NH_2CH_2CH_2 \cdot H_2PO_4$.

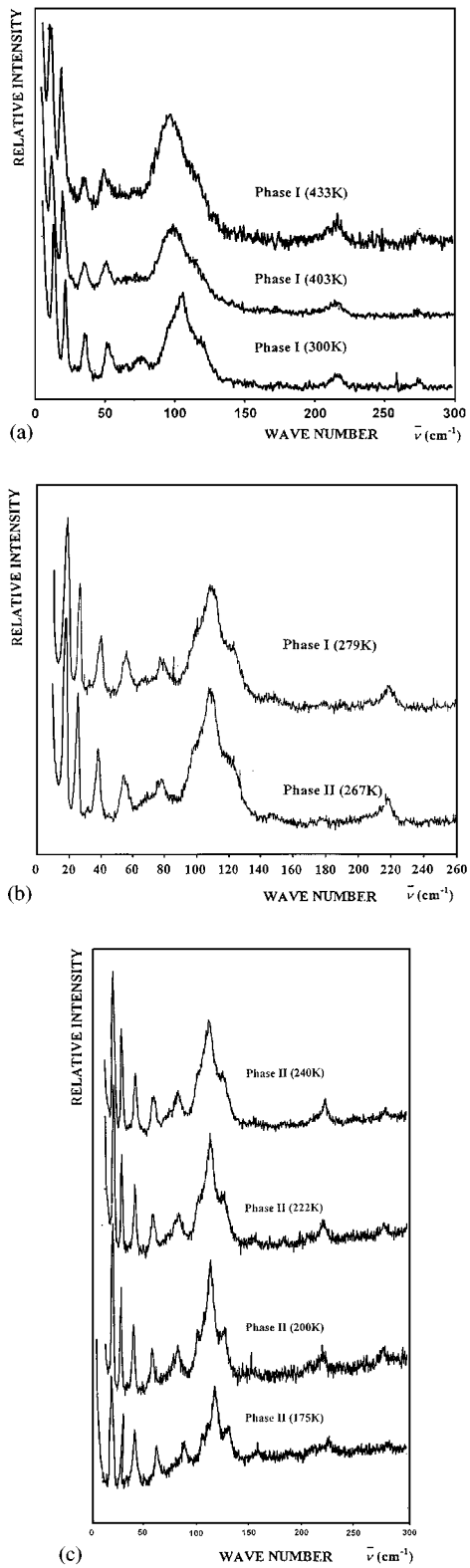

FIG. 4. Raman spectra of $C_6H_5CH_2CHCH_2CH_2NH_2CH_2CH_2 \cdot H_2PO_4$. at low frequency 5–300 cm^{-1} and characterization of the two different phases: (A) 300 K $\leq T \leq$ 433 K, (B) 267 K $\leq T \leq$ 279 K (C) 175 K $\leq T \leq$ 240 K.

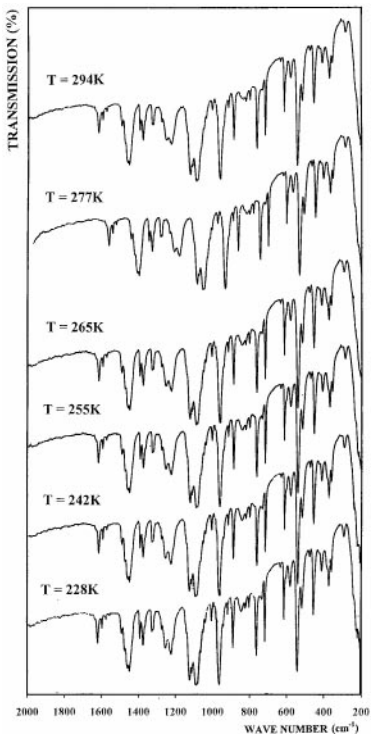

FIG. 5. IR spectra between 2000 and 200 cm^{-1}at different temperatures.

transition at about 270 K. Continuity is also observed for the half widths behavior of the Raman lines versus temperature for the II → I transition. The above result confirms the second-order character of the II → I transition.

The broadness of some bands observed in phases I and II indicates a large amount of disorder. Figure 5 shows the IR spectra of N-BPP at different temperatures in the 2000–200 cm^{-1} range.

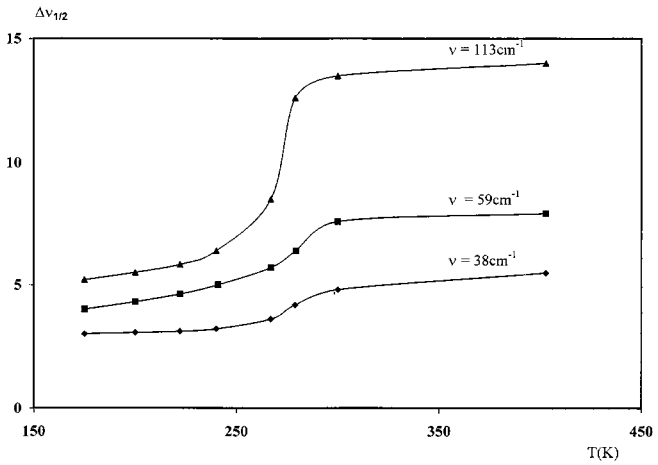

FIG. 6. Halfwidth variations of some Raman bands as function of temperature.

ACKNOWLEDGMENTS

We are grateful to Dr. N. Zouari for his help and Prof. A. Driss for access to the CAD-4 diffractometer.

REFERENCES

1. Z. Elaoud, S. Kamoun, T. Mhiri, and J. Jaud, *J. Chem. Crystallogr.* **29**(5), 541 (1999).
2. S. Kamoun, A. Jouini, M. Kamoun, and A. Daoud, *C. R. Acad. Sci. Paris* **307**(II), 1761 (1988).
3. S. Kamoun, A. Jouini, M. Kamoun, and A. Daoud, *Acta Crystallogr. C* **45,** 81 (1989).
4. S. Kamoun, A. Jouini, A. Daoud, A. Durif, and J. C. Guitel, *Acta Crystallogr. C* **48,** 133 (1992).
5. S. Kamoun, A. Jouini, and A. Daoud, *Acta Crystallogr. C* **47,** 117 (1991).
6. S. Kamoun and A. Jouini, *J. Solid State Chem.* **89,** 67 (1990).
7. S. Kamoun, A. Jouini, and A. Daoud, *Acta Crystallogr. C* **46,** 1481, (1990).
8. S. Kamoun, A. Daoud, A. Elfakir, M. Quarton, and I. Ledoux, *Solid State Commun.* **94,** 893 (1995).
9. Z. Elaoud, S. Kamoun, J. Jaud, and T. Mhiri. *J. Chem. Crystallogr.* **28**(4), 313 (1998).
10. G. Charlot, "Chimie Analytique Quantitative", Vol. II. Masson et cie, Parie, 1974.
11. G. M. Sheldrick, SHELXS 86, Univ. Of Gottingen, Germany, 1990.
12. G. M. Sheldrick, SHELXL 93, Univ. Of Gottingen, Germany, 1993.
13. S. Chaabouni, S. Kamoun, *J. Alloys Compd.* **224,** 207 (1995).
14. A. Lipka, *Z. Anorg. Allg. Chem.* **469,** 218 (1980).
15. A. Lipka and D. Morotz, *Z. Anorg. Allg. Chem.* **440,** 231, (1978).
16. M. Gdaniec, R. Kosturkiewiez, R. Jaknbas, and L. Sobezyk. *Ferroelectrics* **77,** 31 (1988).
17. S. Kamoun, M. Bouachir, A. Daoud, and F. Romain, *Phase Transitions* **44,** 271 (1993).
18. B. Marchon and A. Novak, *J. Chem. Phys.* **5,** 210 (1983).
19. B. Marchon, A. Novak, and R. Blinc, *J. Raman Spectrosc.* **18,** 447 (1987).
20. C. Sourisseau and G. Lucazeau, *J. Raman Spectrosc.* **8,** 311 (1979).
21. N. Toupry-Krauzman, H. Poulet, and M. Lepostollec, *J. Raman Spectrosc.* **8,** 115 (1979).
22. Y. Abid, M. Kamoun, A. Daoud, and F. Romain, *Phase Transitions* **33,** 119 (1991).